Walisongo Journal of Chemistry
**Walisongo Journal of Chemistry Vol. 9 Issue 1 (2026), 76-100**
**ISSN:** 2621-5985 (online); 2549-385X (print)
**DOI:** https://doi.org/10.21580/wjc.v9i1.31732

# MOLECULAR DOCKING AND IN SILICO ANALYSIS OF PSIDIUM GUAJAVA L. LEAF METABOLITES AGAINST PfDHFR AND PfLDH: UNVEILING NEW ANTIMALARIAL CANDIDATES

***Nurcahyo Iman Prakoso[1,4*], Apriyadi Pramana[1,4], Alyaa Nata Cherry Waluyo[1], Gani Purwiandono[1,4], Pinus Jumaryatno[2], Atina Ahdika[3]***

*[1]Department of Chemistry, Faculty of Mathematics and Natural Sciences, Universitas Islam Indonesia, Kampus Terpadu UII, Jl. Kaliurang Km 14, Sleman, Yogyakarta, Indonesia*
*[2]Department of Pharmacy, Faculty of Mathematics and Natural Sciences, Universitas Islam Indonesia, Kampus Terpadu UII, Jl. Kaliurang Km 14, Sleman, Yogyakarta, Indonesia*
*[3]Department of Statistics, Faculty of Mathematics and Natural Sciences, Universitas Islam Indonesia, Kampus Terpadu UII, Jl. Kaliurang Km 14, Sleman, Yogyakarta, Indonesia*
*[4]In Silico Laboratory for Material Innovation and Therapeutics (ILLUMINATE) Research Centre, Universitas Islam Indonesia, Laboratorium Kimia, Kampus Terpadu UII, Jl. Kaliurang Km 14, Sleman, Yogyakarta 55584, Indonesia*

*Corresponding author: nurcahyo.ip@uii.ac.id

***Abstract***

*Resistance of Plasmodium falciparum to conventional antimalarial drugs has created an urgent need for new drug candidates. In this study, six bioactive compounds identified from guava (Psidium guajava L.) leaves, namely quercetin, guaijaverin, 3-tert-butyl-4-methoxyphenol, petasitolone, hyptatic acid, and stigmastane-3,6-dione, were evaluated as potential inhibitors of PfDHFR and PfLDH using in silico approaches, including target identification and validation, molecular docking, binding pocket analysis, and ADMET (Absorption, Distribution, Metabolism, Excretion, and Toxicity) prediction. Both enzymes were highly expressed during the ring stage, essential, non-redundant, and selective toward human homologs, supporting their suitability as antimalarial targets. Molecular docking against PfDHFR revealed that stigmastane-3,6-dione exhibited the strongest binding affinity (−10.4 kcal/mol), followed by guaijaverin (−9.6 kcal/mol) and quercetin (−8.7 kcal/mol), with stable interactions involving key active-site residues. Against PfLDH, quercetin and hyptatic acid showed the best binding affinity (−8.0 kcal/mol), followed by guaijaverin and stigmastane-3,6-dione (−7.7 kcal/mol). However, binding pocket analysis showed that only quercetin, guaijaverin, and petasitolone properly occupied the active binding pocket, whereas hyptatic acid and stigmastane-3,6-dione interacted outside the catalytic site. These findings indicate that quercetin, guaijaverin, and petasitolone may act through competitive inhibition. Molecular dynamics simulation (20 ns) was subsequently performed on selected protein–ligand complexes, in which quercetin and stigmastane-3,6-dione were selected as representative top ligands, while chloroquine was included as a positive control. RMSD, RMSF, and ligand movement analyses demonstrated that quercetin exhibited greater stability in PfLDH than chloroquine. Overall, this study identifies quercetin, guaijaverin, petasitolone, and stigmastane-3,6-dione as promising antimalarial candidates, supported by ADMET predictions showing favorable pharmacokinetic properties and providing a strong rationale for further in vitro and in vivo evaluation.*

***Keywords:*** In Silico*; Antimalarial;* Psidium guajava *L.; PfLDH; PfDHFR*

## Introduction

Malaria remains a serious global health issue, with a high mortality rate that has not shown a significant and sustained decline [1,2]. Although prevention and control efforts continue, an adequate solution has not yet been achieved. The emergence of *Plasmodium falciparum* strains resistant to artemisinin-based combination therapy (ACT) has worsened this situation [3-6]. This resistance is caused by genetic mutations in the Kelch 13 protein and has spread rapidly in Southeast Asia and several regions of Africa, weakening global efforts to combat the disease [7-10]. This condition is further exacerbated by the failure of standard treatments, which threatens the global goal of malaria eradication. Therefore, there is an urgent need to identify innovative chemical compounds with new mechanisms of action that are effective against increasing drug resistance.

Natural product compounds have consistently served as sources of the most effective antimalarial treatments to date, as demonstrated by the discovery of quinine from *Cinchona calisaya* and artemisinin from *Artemisia annua* [11-14]. This potential is attributed to their unique structures and stereochemistry, which are sometimes superior to those of conventional synthetic antimalarial compounds [15-18]. Indonesia possesses extraordinary biodiversity, with more than 30,000 tropical plant species. This enormous potential remains largely untapped and may provide new antimalarial agents. Important information can also be obtained from endemic plants that have been used for generations by local communities to treat malaria fever [19-23].

Drug development from natural products presents significant challenges. It requires not only the identification of biological activity but also an understanding of the mechanism of action of candidate compounds [24-35]. In Indonesia, most research on the antimalarial potential of natural products remains limited to descriptive studies and basic phenotypic testing, resulting in a significant gap in understanding the specific interactions between secondary metabolites and key protein targets in *P. falciparum*. The transition from lead compound discovery to preclinical development requires comprehensive mechanistic studies to overcome obstacles arising from the lack of critical information regarding binding affinity and ligand–receptor stability.

*In silico* methods using molecular docking simulations have transformed drug discovery by efficiently predicting ligand interactions with key target proteins, such as dihydrofolate reductase (DHFR) and lactate dehydrogenase (LDH). This predictive capability allows for critical validation of the antimalarial potential of candidate compounds before laboratory experiments. Molecular docking can provide important insights into the structure–activity relationship between candidate compounds and protein targets. These insights enable targeted compound modification, improve selectivity and potency, and support the development of new and more effective therapies [36-37].

Although several studies have consistently reported the pharmacological benefits of *P. guajava L.* leaves, the focus has largely been limited to quercetin as the primary bioactive compound [38-40]. While *in silico* analyses have effectively examined the interactions of quercetin with various therapeutic targets, other important secondary metabolites from *P. guajava* L. remain largely unexplored and unreported. Therefore, comprehensive *in silico* exploration and evaluation through molecular docking are needed to assess other potential secondary metabolites in *P. guajava L.* leaves. Computational screening can help identify potential novel compounds and provide a more complete understanding of their therapeutic potential



 | ISSN 2621-5985 (online) | ISSN 2549-385X (print)
Volume 9, Nomor 1, 2026

as drug candidates, thereby supporting future drug discovery initiatives.

Based on this background, this study was conducted to evaluate the potential of six active compounds from *P. guajava* L. leaves, namely quercetin, guaijaverin, 3-tert-butyl-4-methoxyphenol, petasitolone, hyptatic acid, and stigmastane-3,6-dione, as antimalarial candidates through *in silico* approaches. These approaches included molecular docking against key protein targets, namely PfDHFR (PDB: 1J3K) and PfLDH (PDB: 1LDG), and ADMET (Absorption, Distribution, Metabolism, Excretion, and Toxicity) prediction analysis to assess pharmacokinetic feasibility. This study is expected to contribute scientifically to the early identification of natural-based antimalarial drug candidates that are safer, more effective, and suitable for further development through *in vitro* and *in vivo* studies.

Although the antimalarial potential of major flavonoids such as quercetin and guaijaverin has been widely reported, a comprehensive understanding of the contribution of other secondary metabolites in *P. guajava* L. to protein targets, particularly PfDHFR and PfLDH, remains limited. This study not only confirms the activity of the main compounds, quercetin and guaijaverin, but also analyzes the antimalarial potential of other pharmacophores, including 3-tert-butyl-4-methoxyphenol, petasitolone, hyptatic acid, and stigmastane-3,6-dione, thereby providing a more holistic profile of potential Plasmodium inhibitor candidates.

## Experimental Section

### Materials

The materials used in this study included the 3D crystal structures of *P. falciparum* proteins, namely PfDHFR (PDB: 1J3K) and PfLDH (PDB: 1LDG), obtained from the Protein Data Bank (www.rcsb.org). Compounds identified from *P. guajava* L. leaves in previous research [27], namely quercetin, guaijaverin, 3-tert-butyl-4-methoxyphenol, petasitolone, hyptatic acid, stigmastane-3,6-dione, and chloroquine, were used in this *in silico* study. Chloroquine was used as an antimalarial control. The 3D structures of these compounds were obtained from PubChem (https://pubchem.ncbi.nlm.nih.gov/) and ChemSpider (www.chemspider.com). This study was conducted using PyRx 1.0 and Discovery Studio 2025 software.

### Instruments

The hardware used in this study consisted of a Veritron M PC with an Intel Core i7-12700 processor, 32 GB RAM, 1 TB SSD, 2 GB VGA, 23.8-inch display, LAN, Wi-Fi, Bluetooth, DVDRW, 500 W PSU, and Windows 11 Home.

### Procedure

### Target Identification and Validation

Target identification and validation were conducted to ensure that the selected targets are essential for *P. falciparum* during the asexual phase. The essentiality of each selected target was evaluated to determine its significance for *P. falciparum*. This assessment involved analyzing target gene expression profiles using the Plasmodium Genomics Resource Database (PlasmoDB; https://plasmodb.org/plasmo/app) and TDR Targets (https://tdrtargets.org/), with particular emphasis on expression during the ring stage of the parasite life cycle. Furthermore, gene knockout data were examined using PhenoPlasm (https://phenoplasm.org/) to determine whether *P. falciparum* viability is compromised in the absence of the target.

Redundancy analysis was then performed to determine whether *P. falciparum* has proteins similar to the selected target. If similar proteins exist, the target may be considered less essential because the loss of that protein could be compensated for by another protein with a similar structure and function. Targets that passed the redundancy analysis were subsequently evaluated for selectivity to determine their similarity to human proteins. Selectivity analysis was conducted

by submitting the target sequences to the Basic Local Alignment Search Tool for proteins (BLASTp) at https://blast.ncbi.nlm.nih.gov/Blast.cgi. Searches were performed using the following filters: organism, *Homo sapiens*; percent identity, 30–100%; E-value, 1e−4 to 1e−3; and query coverage, 30–100%.

**Bioactivity Prediction Analysis**

Antimalarial bioactivity prediction was performed using PASS Online (Prediction of Activity Spectra for Substances; http://way2drug.com/passonline) to preliminarily evaluate the biological activity potential of the dominant compounds identified from the *n*-hexane fraction of *P. guajava* L. leaves. The prediction results were assessed based on the probability of activity (Pa) and probability of inactivity (Pi), with chloroquine used as a positive control for comparison.

**Molecular Docking Analysis**

The 3D ligand structures obtained from PubChem and ChemSpider, namely quercetin, guaijaverin, 3-tert-butyl-4-methoxyphenol, petasitolone, hyptatic acid, stigmastane-3,6-dione, and chloroquine, were prepared using PyRx 1.0, optimized, and converted into docking format (.pdbqt). The 3D target structures obtained from the Protein Data Bank, namely PfDHFR (PDB: 1J3K) and PfLDH (PDB: 1LDG), were prepared by removing water molecules and other non-essential molecules, leaving only the target protein structures.

Molecular docking was carried out using blind docking with AutoDock Vina, with an exhaustiveness parameter of 126. Validation was performed by re-docking target protein structures containing native ligands. The molecular docking protocol was considered valid if the root-mean-square deviation (RMSD) value obtained from re-docking was less than 2 Å. Protein–ligand interactions were visualized using Discovery Studio 2025, focusing on the pose with the lowest binding affinity. The docking results were also used to predict binding pockets using DoGSiteScorer [41-42] to verify whether the docking positions were accurate, as false-positive results may occur when molecular docking indicates good binding affinity but the ligand is located in an incorrect position that does not interfere with target function.

**ADMET Prediction**

Compounds with favorable interactions with PfDHFR (PDB: 1J3K) and PfLDH (PDB: 1LDG) were subjected to ADMET prediction to determine their potential as drug candidates. This prediction was performed using several web servers by inputting the SMILES format of each compound. The web servers used were pkCSM (https://biosig.lab.uq.edu.au/pkcsm/) and ProTox 3.0 (https://tox.charite.de/protox3/) [43].

**Molecular Dynamics**

Molecular dynamics (MD) simulations were performed using YASARA to evaluate the stability of the protein–ligand complexes obtained from molecular docking under conditions that mimic the physiological environment. The protein structures, PfDHFR and PfLDH, and their corresponding ligands were selected from the best docking results based on binding affinity and proper positioning within the active binding site. Prior to simulation, each complex was prepared by removing non-essential molecules, followed by structural cleaning and assignment of protonation states at physiological pH (7.4).

The hydrogen-bonding network was optimized to ensure realistic interaction geometry. The AMBER14 force field was applied to describe molecular interactions within the system. Each complex was placed in a cubic simulation box with an extension of 10 Å and solvated with water molecules. The system was neutralized by adding $Na^+$ and $Cl^-$ ions at a physiological concentration of 0.9%. Periodic boundary conditions were applied, and long-range electrostatic interactions were treated using the Particle Mesh Ewald method with an 8 Å cut-off. Pressure control was maintained based on

solvent density, and the simulation temperature was set to 298 K. Energy minimization was conducted to remove steric clashes, followed by an equilibration phase. Production MD simulations were then carried out for 20 ns. The resulting trajectories were analyzed to evaluate the stability of the complexes using RMSD and RMSF parameters.

## Results and Discussion

### Target Identification and Validation

The analysis indicated that PfDHFR was expressed at levels of 40–60% during the ring stage, classifying it as having intermediate expression (see **Table 1**). This expression indicates that PfDHFR contributes to the early developmental phase of the parasite, although not at its maximum capacity. Importantly, this enzyme remains a critical target because the ring stage, as a developmental stage of *P. falciparum*, is crucial for DNA replication and is associated with an increased demand for folate metabolism. In contrast, PfLDH exhibited expression levels of 80–100%, indicating very high expression. This demonstrates its dominance and critical role as a metabolic component during the ring stage. The enzymatic activity and role of PfLDH are crucial because they are linked to anaerobic glycolysis, the primary pathway for energy production in *P. falciparum*. The very high expression of PfLDH reflects the parasite's dependence on this enzyme, and inhibition of PfLDH may have rapid and lethal effects on the parasite. Collectively, these findings underscore the importance of both targets for *P. falciparum* survival.

The PfDHFR and PfLDH enzymes are classified as refractory targets based on CRISPR and genetic interference experiments, indicating that genetic deletion of these enzymes is highly difficult. This implies that these enzymes are essential and that their loss would significantly disrupt the *Plasmodium* life cycle. From a pharmacological perspective, refractory targets are considered crucial for drug development because their inhibition can disrupt vital biological functions of the target parasite, *P. falciparum*. Therefore, natural compounds with active inhibitory activity against these enzymes and low toxicity toward humans may provide strong antiparasitic effects.

**Table 1**. Essentiality analysis of PfDHFR and PfLDH

| Target | Expression in the Ring Phase (%) | Disruptability | Redundancy | Selectivity Toward Humans |
|---|---|---|---|---|
| PfDHFR | 40-60 (Intermediate) | Refractory | No | Yes |
| PfLDH | 80-100 (Very High) | Refractory | No | Yes |

Neither PfDHFR nor PfLDH exhibited functional redundancy, indicating that there are no alternative or backup enzymatic pathways that can replace the loss of these enzymes in the *P. falciparum* metabolic pathway. This strongly suggests that inhibition of these targets would likely lead to fatal metabolic failure. The absence of alternative pathways in folate metabolism supports the activity of inhibitors such as pyrimethamine. Similarly, for PfLDH, the parasite is highly dependent on glycolysis for energy production, and deficiency of this enzyme would pose a serious problem for parasite survival. Therefore, targeting these enzymes represents an attractive, effective, and efficient strategy in the drug discovery process.

Both targeted enzymes exhibit significant functional and structural differences compared with their human homologs, enabling the development of safe, specific, and highly selective drugs against the parasite. In addition, BLASTp analysis

revealed no significant homology with human proteins within the applied E-value cutoff range of 1e−4 to 1e−3, indicating high selectivity and suggesting a minimal risk of off-target effects in human systems. Importantly, structural differences in the active-site residues of PfDHFR in *P. falciparum* facilitate the specific design of inhibitors. Furthermore, the presence of a unique loop region in PfLDH, which is absent in human LDH, may allow for the development of selective inhibitors. These differences minimize the risk of side effects and may provide non-toxic therapeutic effects on human cells.

Based on the analysis of PfDHFR and PfLDH, including their susceptibility to interference, redundancy, and selectivity, both enzymes meet important pharmacological and biological criteria as valid drug targets. Their low redundancy and high selectivity make them suitable targets for drug development. Furthermore, the importance of both enzymes, accompanied by their high levels of expression in parasite metabolism, demonstrates their crucial role. Inhibition of these enzymes is likely to kill *P. falciparum,* making them highly suitable targets for molecular docking and the development of new drug designs aimed at identifying effective antimalarial compounds.

**Bioactivity Prediction Analysis**

Prediction of antimalarial bioactivity was performed using PASS Online to provide preliminary screening of dominant compounds identified from the *n*-hexane fraction of *P. guajava* L. leaves prior to structure-based analysis. The prediction results were compared with chloroquine as a positive control by evaluating the probability of activity (Pa) and probability of inactivity (Pi) (see **Table 2**).

The prediction results showed that 3-tert-butyl-4-methoxyphenol, petasitolone, and stigmastane-3,6-dione exhibited Pa values greater than Pi values, indicating that these compounds retain potential antimalarial activity despite relatively low prediction confidence (Pa < 0.7). According to the PASS interpretation, compounds with Pa values below 0.7 may still demonstrate biological activity but often represent structurally novel compounds that are less similar to compounds already available in the PASS database. This phenomenon is commonly observed in natural products that possess unique chemical scaffolds and mechanisms of action.

**Table 2.** Probability of activity (Pa) and probability of inactivity (Pi) of compounds from the n-hexane fraction of P. guajava L.

| Compound | Antimalaria | |
|---|---|---|
| | Pa | Pi |
| *3-tert-Butyl-4-methoxyphenol* | 0.183 | 0.074 |
| *Guaijaverin* | 0.473 | 0.004 |
| *Quercetin* | 0.365 | 0.008 |
| *Petasitolone* | 0.193 | 0.064 |
| *Hyptatic acid* | N/A | N/A |
| *Stigmastane-3,6-dione* | 0.180 | 0.078 |
| *Chloroquine* | 0.898 | 0.002 |

Petasitolone and 3-tert-butyl-4-methoxyphenol showed slightly higher Pa values than stigmastane-3,6-dione, which may be attributed to the presence of oxygen-containing functional groups that are more commonly found in known bioactive compounds. In contrast, stigmastane-3,6-dione has a rigid steroidal framework that may be underrepresented in the PASS reference dataset, resulting in a lower predicted probability despite its potential biological relevance. Hyptatic acid was not detected in the PASS database, suggesting limited structural reference data for this triterpenoid compound and highlighting the novelty of its chemical scaffold.

Meanwhile, chloroquine demonstrated a significantly higher Pa value (0.898), indicating strong structural similarity to previously reported antimalarial compounds and validating the reliability of the prediction model. Although the *P. guajava* L. leaf metabolites showed lower PASS prediction scores than

chloroquine, this does not eliminate their antimalarial potential. Therefore, further computational approaches, including molecular docking, binding pocket validation, molecular dynamics simulation, and ADMET analysis, were necessary to comprehensively evaluate their inhibitory potential against PfDHFR and PfLDH.

**Molecular Docking Analysis Against PfDHFR**

The results of molecular docking of compounds contained in *P. guajava* L. leaves against the PfDHFR enzyme are presented in **Figure 1** and **Table 3**. Several metabolite compounds showed significant antimalarial potential, as indicated by their binding energy values and important interactions within the enzyme active site. Stigmastane-3,6-dione showed the lowest binding energy at −10.4 kcal/mol, followed by guaijaverin at −9.6 kcal/mol and quercetin at −8.7 kcal/mol. These compounds interacted with key residues such as Tyr170, Cys15, Ile14, Ser111, and Gly41, which are important for the stability of the enzyme–ligand complex, particularly during ligand binding.

In **Figure 1(a,b)**, guaijaverin forms hydrogen-bond interactions with Ile14, Ser111, and Tyr170 in the substrate-binding pocket, supported by hydrophobic contacts with Leu46, Leu40, Gly41, and Ile112. The combination of hydrophobic and polar interactions contributes to strong complex stability, consistent with its low binding energy of −9.6 kcal/mol. Guaijaverin shows competitive inhibitor characteristics, mainly by occupying and stabilizing the hydrophobic region of the enzyme pocket.

**Figure 1(c,d)** presents the interaction profile of quercetin, which also shows strong binding affinity (−8.7 kcal/mol). The interactions included hydrogen bonds with Gly44, Ser111, and Tyr170, followed by hydrophobic contacts involving Leu46, Val195, Leu40, and Gly41. This pattern is consistent with the profile of quercetin as a flavonoid compound, in which the phenolic groups and aromatic rings enable hydrogen-bonding and π–π stacking interactions, with Tyr170 playing an important role in stabilizing the bond between the ligand and the active site.

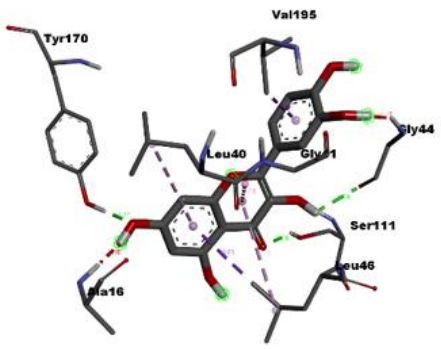


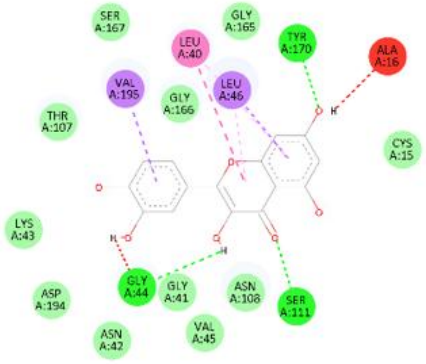


(a)



Copyright © 2026 WJC | ISSN 2621-5985 (online) | ISSN 2549-385X (print)
Volume 9, Nomor 1, 2026

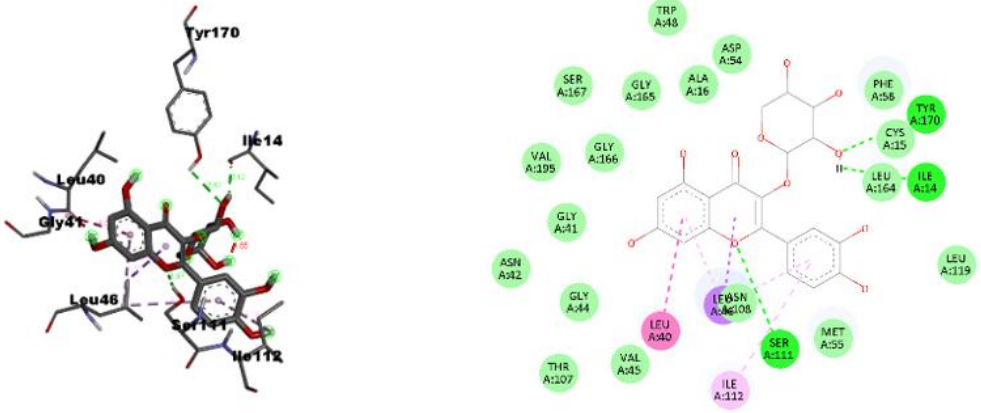


(b)

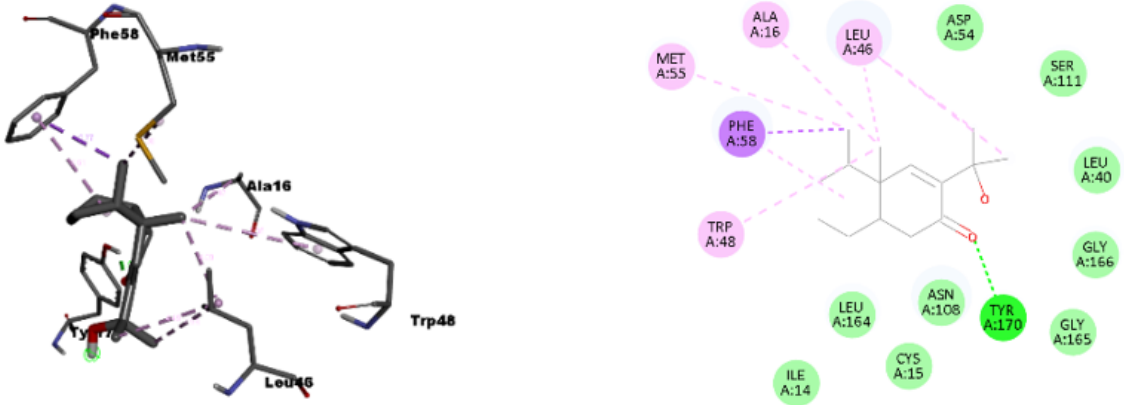


(c)

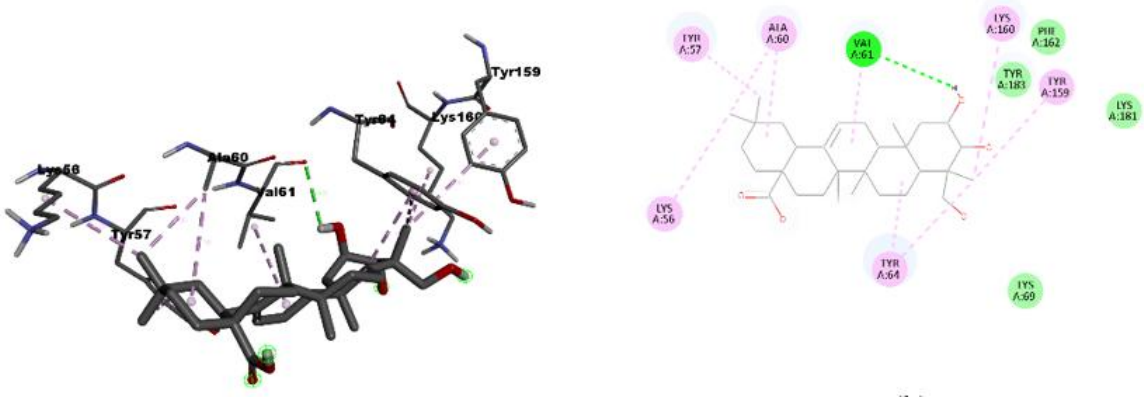


(d)

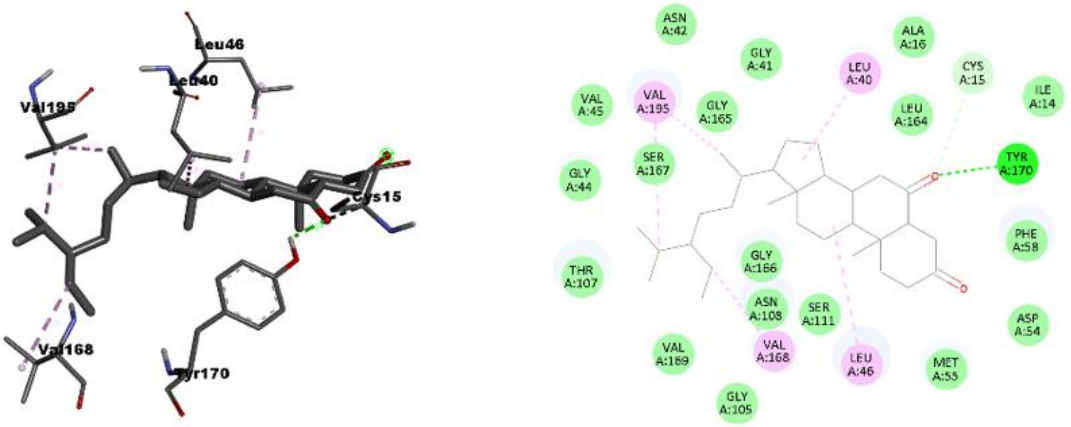


(e)

**Figure 1**. Affinity and binding interactions between PfDHFR and metabolite compounds: quercetin (a), guaijaverin (b), petasitolone (c), hyptatic acid (d), and stigmastane-3,6-dione (e).

Stigmastane-3,6-dione, a steroid metabolite or, more precisely, a phytosterol derivative, emerged as the most potent ligand, with a binding energy of −10.4 kcal/mol (see **Figure 1i,j**). This compound forms hydrogen-bond interactions with Tyr170 and Cys15 and engages in hydrophobic interactions with Leu46, Val195, Val168, and Leu40. In other words, this ligand is capable of occupying the hydrophobic core of PfDHFR. The rigid sterol structure of stigmastane-3,6-dione allows optimal occupancy of the hydrophobic pocket, resulting in extensive and stable interactions between the ligand and the target enzyme.

A different pattern was observed for hyptatic acid, which showed only moderate binding affinity, with a binding energy of −7.1 kcal/mol, and formed hydrogen bonds only with Val61 (see **Figure 1g,h**). Although it was able to form extensive hydrophobic contacts with Lys160, Lys56, Ala60, Val61, Tyr57, Tyr64, and Tyr159, contributing to complex stabilization, this ligand did not interact directly with the catalytic residue. This may be due to the large multi-ring structure of hyptatic acid, which results in a shallower interaction depth compared with the more potent ligands discussed above.

Petasitolone, a terpenoid compound, also exhibited behavior similar to that of hyptatic acid, showing only moderate activity with a binding energy of −7.6 kcal/mol (see **Figure 1e,f**). Its rigid, non-planar cyclic structure resulted in interactions that were not as extensive as those of the stronger ligands. Its interaction profile included hydrogen bonds with Tyr170 and hydrophobic contacts with Phe58, Ala16, Leu46, Met55, and Trp48.

**Table 3.** Molecular docking analysis results for the active site of the PfDHFR enzyme (PDB code: 1J3K)

| Compound | Structure | Binding Affinity (kcal/mol) | Type of Interaction | | |
|---|---|---|---|---|---|
| | | | H-Bond | Hydrophobic | Others |
| Chloroquine (PubChem CID 2719) | 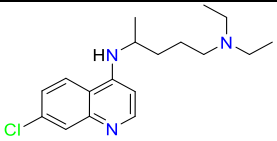 | -7.1 | Asn108, Ser111, Pro113 | Ile112, Leu119, Leu164, Ala16, Leu46, Trp48, Phe58, Phe116 | - |

| | | | | | |
|---|---|---|---|---|---|
| Quercetin (PubChem CID 5280343) | 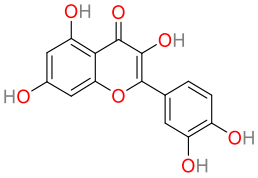 | -8.7 | Gly44, Ser111, Tyr170 | Leu46, Val195, Leu40, Gly41 | - |
| Guaijaverin (PubChem CID 5481224) | 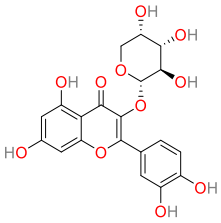 | -9.6 | Ile14, Ser111, Tyr170 | Leu46, Leu40, Gly41, Ile112 | - |
| 3-tert-Butyl-4-methoxyphenol (PubChem CID 6932) | 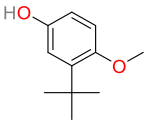 | -5.8 | Asp54 | Phe58, Ile112 | - |
| Petasitolone (PubChem CID 5320506) | 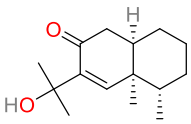 | -7.6 | Tyr170 | Phe58, Ala16, Leu46, Met55, Trp48 | - |
| Hyptatic acid (PubChem CID 12305222) | 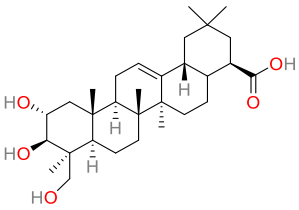 | -7.1 | Val61 | Lys160, Lys56, Ala60, Val61, Tyr57, Tyr64, Tyr159 | - |
| Stigmastane-3,6-dione (PubChem CID 13992092) | 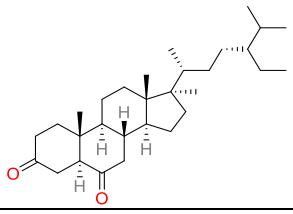 | -10.4 | Tyr170, Cys15 | Leu46, Val195, Val168, Leu40 | - |

Molecular docking analysis of PfDHFR revealed that the binding energy of chloroquine, a positive control and conventional drug still in use, was higher than those of guaijaverin, quercetin, and stigmastane-3,6-dione, indicating lower inhibitory potential than these three compounds. Stigmastane-3,6-dione stood out as the most potent inhibitor due to its lowest binding energy and extensive interactions with key residues. Guaijaverin and quercetin also exhibited significant inhibitory potential by consistently engaging essential amino acids required for enzyme inhibition. Overall, petasitolone demonstrated potential as a competitive PfDHFR inhibitor through a combination of hydrogen bonding and hydrophobic interactions. These findings support the prospect that bioactive compounds from *P. guajava* L. can serve as promising lead candidates in the development of antimalarial agents targeting PfDHFR.

## Molecular Docking Analysis Against PfLDH

The results of molecular docking of compounds contained in *P. guajava* L. leaves against PfLDH are presented in **Figure 2** and **Table 4**. Based on the molecular interaction analysis of PfLDH, quercetin and hyptatic acid emerged as the most potent inhibitor candidates, with the strongest binding energy of −8.0 kcal/mol. Quercetin acted through hydrogen-bond formation with Gly99, Asn140, and Thr139, supported by π−π stacking interactions typical of flavonoids, thereby disrupting the stability

of the enzymatic transition state. Meanwhile, hyptatic acid demonstrated similar effectiveness through deeper penetration into the active pocket, where its large triterpenoid structure formed an extensive hydrophobic interaction network with residues such as Val200 and a stable hydrogen bond with Asp230.

Guaijaverin and stigmastane-3,6-dione also showed significant potential, with binding energies of −7.7 kcal/mol. Guaijaverin effectively competed in the catalytic region through hydrogen bonding with critical residues such as Gly99 and Asp53, which regulate pyruvate binding. Stigmastane-3,6-dione utilized its rigid sterol structure to form hydrophobic anchoring in the enzyme pocket, despite forming only one hydrogen bond with Arg185. Overall, these natural compounds showed better affinity than the positive control chloroquine (−6.4 kcal/mol) and petasitolone (−5.8 kcal/mol), thus strengthening the possibility of developing natural products, especially from *P. guajava* L., as new selective antimalarial agents [44]. Guaijaverin (see **Figure 2c,d**) formed hydrogen-bond interactions with Gly99, Asp53, Ile54, and Thr97, which are residues involved in regulating the binding of pyruvate and the NADH cofactor, and hydrophobic interactions with Ile54, Ile119, Phe100, and Ala98. Meanwhile, quercetin (see **Figure 2a,b**), which was among the most potent compounds, showed hydrogen-bond interactions with Gly99, Asn140, and Thr139 and hydrophobic interactions involving Thr101, Ile31, and Pro250. These interactions are characteristic of flavonoid compounds that contain aromatic and phenolic groups, enabling hydrogen bonding and π–π stacking with aromatic residues in the PfLDH binding pocket. Interactions with Gly99 and Asn140, which are located near the substrate-binding loop, indicate the high potential of quercetin to disrupt the stability of the enzymatic transition state.

Stigmastane-3,6-dione (see **Figure 2g,h**) formed a single hydrogen-bond interaction with Arg185, a key residue in the PfLDH pocket, and hydrophobic interactions with Tyr174, Ile239, Ala249, and Arg171. Its rigid and bulky sterol structure allowed this compound to optimally occupy the hydrophobic pocket of PfLDH and produce strong binding, although not as strong as that of quercetin. The performance of this compound indicates its potential as a PfLDH inhibitor through a hydrophobic interaction mechanism.

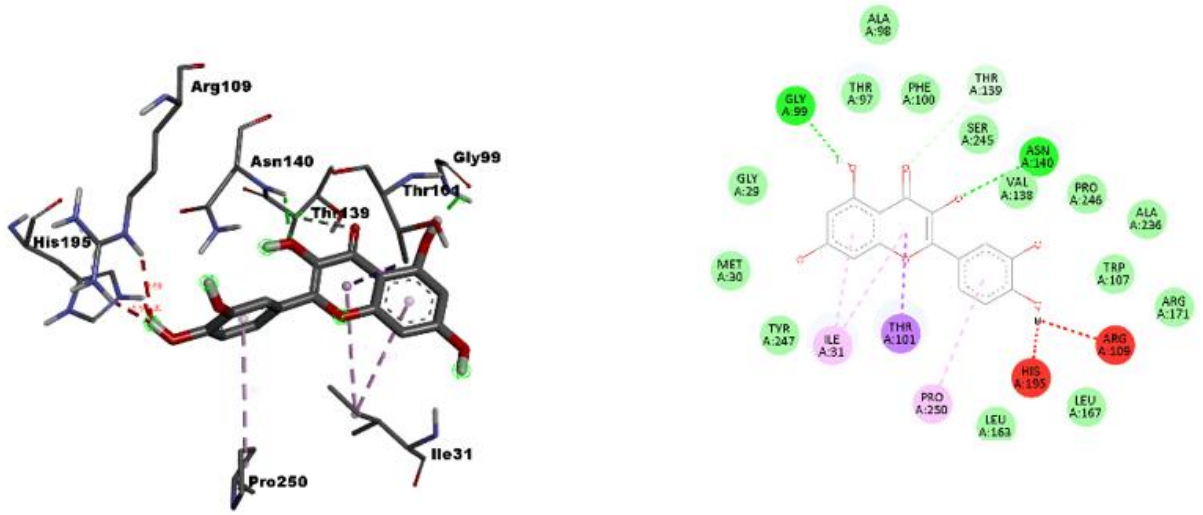


(a)

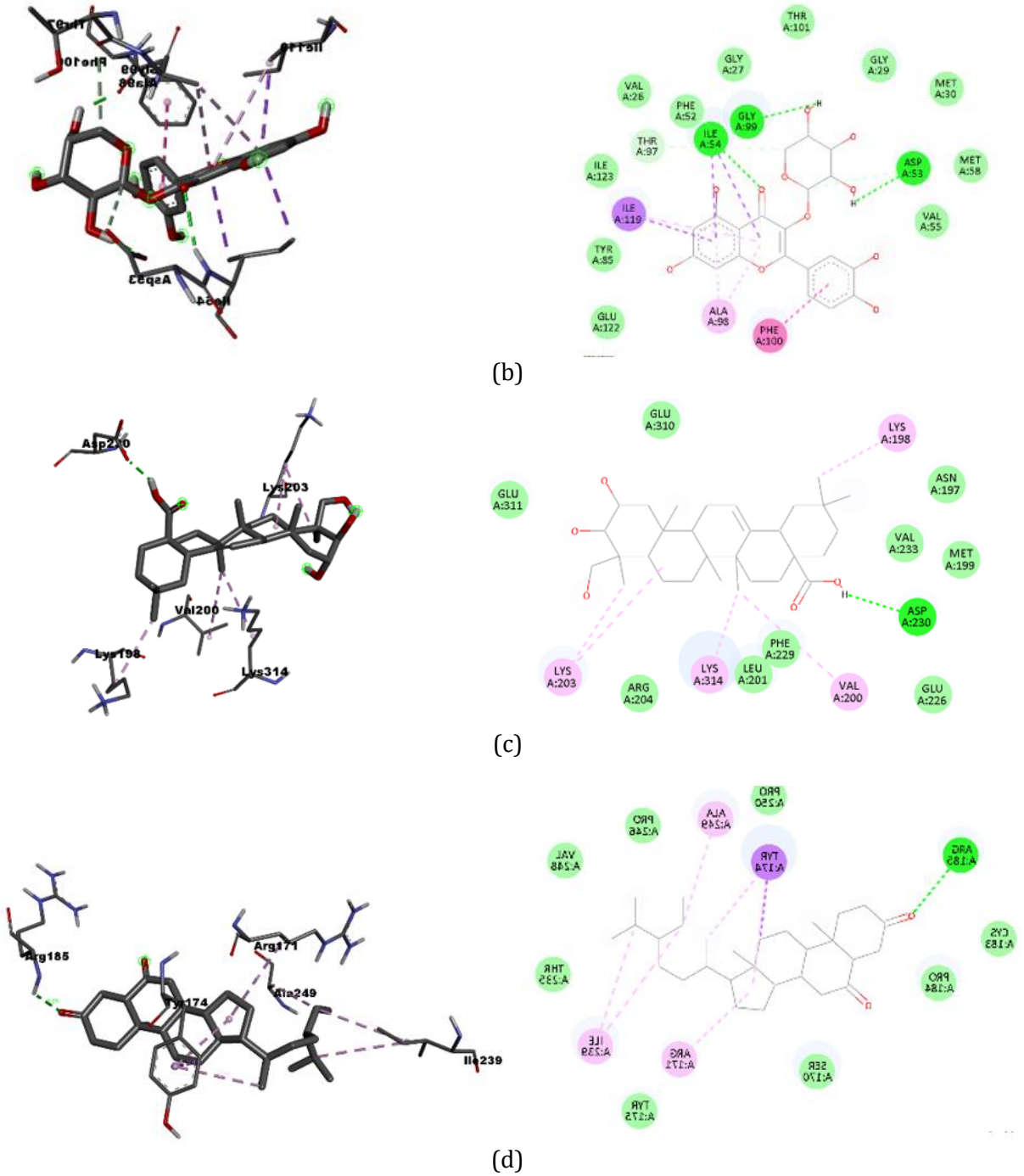


**Figure 2.** Affinity and binding interactions between PfLDH and metabolite compounds: quercetin (a), guaijaverin (b), hyptatic acid (c), and stigmastane-3,6-dione (d)

Hyptatic acid (see **Figure 2e,f**) exhibited hydrogen-bond interactions with Asp230, which is located at the base of the PfLDH active pocket, and hydrophobic interactions with Val200, Lys314, Lys203, and Lys198, suggesting that this large triterpenoid structure interacts with the hydrophobic surface of the pocket. Its ability to penetrate more deeply into the pocket than petasitolone resulted in stronger affinity, making hyptatic acid comparable to quercetin, although through a different pocket-penetration mechanism. However, despite its favorable docking affinity, subsequent binding pocket analysis revealed that hyptatic acid was positioned

outside the primary catalytic site of PfLDH. This suggests that the observed docking score may represent a false-positive interaction, as strong binding affinity does not always indicate effective competitive inhibition when the ligand fails to occupy the functional active site.

In contrast, compounds such as 3-tert-butyl-4-methoxyphenol (−5.5 kcal/mol), petasitolone (−5.8 kcal/mol), and the positive control chloroquine (−6.4 kcal/mol) exhibited lower affinity, despite interacting with key residues such as Asp53, Phe52, and Ile119, making them less suitable as PfLDH inhibitors.

**Table 4.** Molecular Docking Analysis Results for the Active Site of the PfLDH Enzyme (PDB code: 1LDG)

| Compound | Structure | Binding Affinity (kcal/mol) | Type of Interaction | | |
|---|---|---|---|---|---|
| | | | H-Bond | Hydrophobic | Others |
| Chloroquine (PubChem CID 2719) | 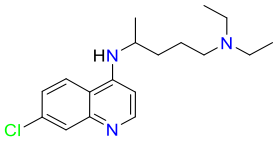 | -6.4 | - | Met30, Ile31, Ile54, Ala98, Ile119 | - |
| Quercetin (PubChem CID 5280343) | 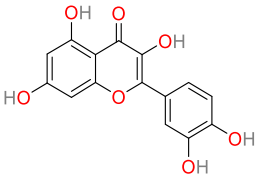 | -8.0 | Gly99, Asn140, Thr139 | Thr101, Ile31, Pro250 | - |
| Guaijaverin (PubChem CID 5481224) | 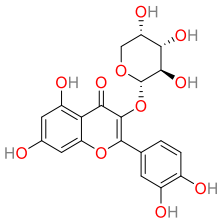 | -7.7 | Gly99, Asp53, Ile54, Thr97 | Ile54, Ile119, Phe100, Ala98 | - |
| 3-tert-Butyl-4-methoxyphenol (PubChem CID 6932) | 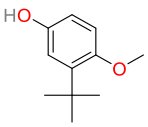 | -5.5 | Phe52, Glu122, Asp53 | Ile54, Ala98, Ile119 | - |
| Petasitolone (PubChem CID 5320506) | 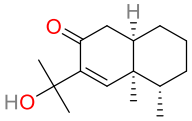 | -5.8 | Met199, Val200 | Lys198, Lys314, Leu201, Phe229 | - |
| Hyptatic acid (PubChem CID 12305222) | 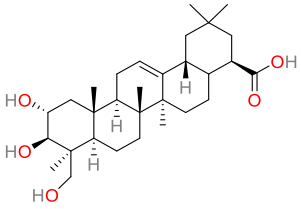 | -8.0 | Asp230 | Val200, Lys314, Lys203, Lys198 | - |

| | | | | | |
|---|---|---|---|---|---|
| Stigmastane-3,6-dione (PubChem CID 13992092) | 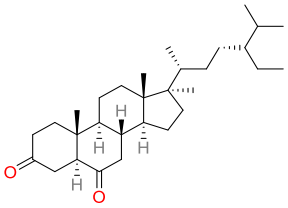 | -7.7 | Arg185 | Tyr174, Ile239, Ala249, Arg171 | - |

**PfDHFR Binding Pocket Analysis**

Binding pocket detection analysis of PfDHFR showed that the inhibitory effectiveness of the test compounds was largely determined by their ability to occupy the primary catalytic site, marked in yellow in **Figure 3**. Stigmastane-3,6-dione emerged as the most promising candidate because its large and rigid sterol structure allowed maximum spatial occupancy within the active site. This finding is consistent with the lowest binding energy obtained in the docking study, indicating a highly stable competitive inhibition mechanism. Similarly, quercetin and guaijaverin also fully occupied the active site, with molecular orientations parallel to the contour of the catalytic site, thereby strongly inhibiting dihydrofolate substrate binding through direct competition with the native ligand.

Petasitolone also showed potential inhibition through direct competition, but with more moderate affinity due to its less optimal penetration depth compared with the other key compounds. Conversely, hyptatic acid exhibited different behavior because it did not fully occupy the active site and tended to interact peripherally or outside the catalytic site. This finding explains why the contribution of hyptatic acid to PfDHFR inhibition was lower and suggests that it may act through a non-competitive mechanism or peripheral stabilization. Overall, these findings prioritize compounds that interact directly within the active site for further ADMET evaluation to assess their pharmacokinetic and safety feasibility as potential antimalarial agents.

Therefore, this analysis indicates that four metabolite compounds from *P. guajava* L., namely quercetin, guaijaverin, petasitolone, and stigmastane-3,6-dione, have potential as antimalarial agents because they can interact directly within the active binding pocket of PfDHFR and inhibit the enzyme through a competitive mechanism with the native ligand. In contrast, hyptatic acid is less potent because it does not occupy the active pocket. Based on these findings, compounds that fit the size and active site of the PfDHFR binding pocket should be prioritized for further evaluation through ADMET prediction to assess their pharmacokinetic feasibility and safety.

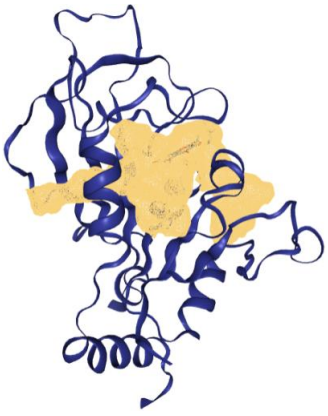

(a)

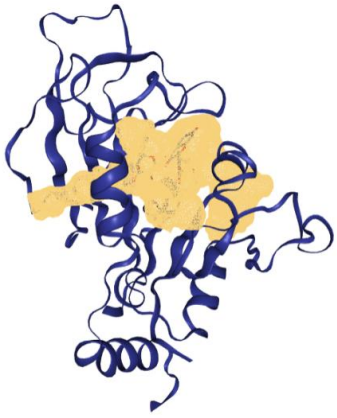

(b)

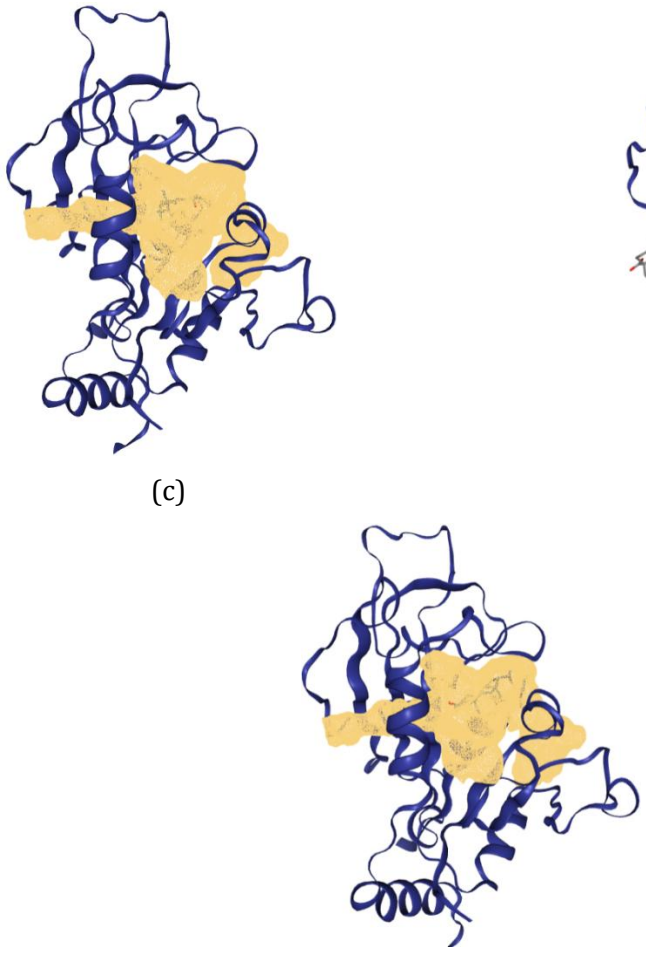

(c) (d)

(e)

**Figure 3.** PfDHFR binding pocket with quercetin (a), guaijaverin (b), petasitolone (c), hyptatic acid (d), and stigmastane-3,6-dione (e).

## PfLDH Binding Pocket Analysis

(a) (b)



Copyright © 2026 WJC | ISSN 2621-5985 (online) | ISSN 2549-385X (print)
Volume 9, Nomor 1, 2026

(c) (d)

**Figure 4.** PfLDH binding pocket with quercetin (a), guaijaverin (b), hyptatic acid (c), and stigmastane-3,6-dione (d).

Binding pocket detection analysis of PfLDH indicated that the inhibitory effectiveness of a compound depends largely on its ability to occupy the key catalytic site, marked in yellow, which serves as the binding site for the substrate pyruvate and the cofactor NADH (see **Figure 4**). Based on ligand positioning, quercetin and guaijaverin emerged as the most potent competitive inhibitor candidates. Quercetin was precisely oriented along the contours of the active site, while guaijaverin adapted its large glycosidic structure to interact directly with key residues within the catalytic site. Petasitolone was also detected within the active site, but with a shallower penetration depth, indicating more moderate affinity and inhibitory efficiency than those of the previous two compounds.

In contrast, hyptatic acid and stigmastane-3,6-dione did not occupy the key active site, thus classifying their interaction mechanisms as non-competitive or peripheral. Hyptatic acid tended to interact in the outer region of the enzyme, while the large and rigid sterol structure of stigmastane-3,6-dione prevented it from fitting into the narrow catalytic cleft. Therefore, its contribution to the inhibition of the main PfLDH pathway is presumed to be limited. These findings strategically prioritize quercetin, guaijaverin, and petasitolone for further ADMET evaluation to ensure their pharmacokinetic and safety feasibility as new antimalarial agent candidates.

Moreover, these binding pocket detection results indicate that quercetin, guaijaverin, and petasitolone can bind directly within the active pocket of PfLDH and potentially inhibit the enzyme through a competitive mechanism. In contrast, hyptatic acid and stigmastane-3,6-dione do not fit into the active pocket; therefore, their interaction mechanism with PfLDH is likely non-competitive and may make only a limited contribution to enzyme inhibition. Based on these findings, only compounds occupying the active binding pocket of PfLDH were prioritized for further analysis as antimalarial candidates. Quercetin was prioritized for molecular dynamics simulation because it demonstrated both strong binding affinity and correct occupation of the catalytic pocket. Guaijaverin was not selected for molecular dynamics despite favorable active-site binding because quercetin exhibited slightly stronger binding affinity and a more favorable interaction profile with critical catalytic residues. Meanwhile, chloroquine was included as a positive control to compare the dynamic stability of quercetin with that of a clinically established antimalarial compound.

**ADMET Prediction**

Pharmacokinetic analysis of the four test compounds provided critical insights into their drug-likeness profiles and therapeutic potential. From a physicochemical perspective, wide variation in lipophilicity (Log P) was observed, ranging from 0.10 to 7.49. The higher

topological polar surface area (TPSA) values of quercetin and guaijaverin indicated better solubility but may limit their cell membrane permeability. Conversely, stigmastane-3,6-dione was characterized by high lipophilicity and a low TPSA value, although it violated some standard drug-likeness criteria (see **Table 5**).

In the absorption and distribution phases, quercetin and petasitolone demonstrated superior water solubility, which may positively influence their bioavailability. Although human intestinal absorption (HIA) was generally moderate to high for all compounds, only petasitolone and stigmastane-3,6-dione showed adequate cellular permeability based on Caco-2 permeability. The blood–brain barrier (BBB) permeability values varied among compounds, with petasitolone showing the highest value, suggesting better potential for BBB penetration than the other compounds.

Metabolism data for guaijaverin, petasitolone, and stigmastane-3,6-dione indicated that these compounds were inactive as inhibitors of the main cytochrome P450 (CYP) enzymes, including CYP2D6, CYP2E1, CYP2C9, CYP2C19, and CYP1A2. However, petasitolone was active against CYP3A4, while quercetin was active against CYP2C9, CYP2C19, and CYP1A2. This suggests that several compounds may have a relatively low likelihood of drug interactions due to enzyme inhibition, although quercetin and petasitolone require closer consideration. Inactivity toward major CYP enzymes is generally a favorable trait for drug candidates because it reduces the risk of adverse metabolic interactions when taken with other medications.

**Table 5**. ADMET Results

| **Pharmacokinetic Parameter** | Quercetin (PubChem CID 5280343) | Guaijaverin (PubChem CID 5481224) | Petasitolone (PubChem CID 5320506) | Stigmastane-3,6-dione (PubChem CID 13992092) |
|---|---|---|---|---|
| **Drug-likeness** | | | | |
| Molecular weight (g/mol) | 302.24 | 434.35 | 236.36 | 428.70 |
| Log P | 1.99 | 0.10 | 3.10 | 7.49 |
| H-bond donor | 5 | 7 | 1 | 0 |
| Topological polar surface area (Å²) | 131.36 | 190.28 | 28.16 | 34.14 |
| Rotatable bonds | 1 | 3 | 1 | 6 |
| **Absorption** | | | | |
| Water solubility (log mol/L) | -2.87 | -3.07 | -3.61 | -6.536 |
| HIA (%) | 74.80 | 49.49 | 94.06 | 97.42 |
| Caco-2 permeability (cm/s) | -0.30 | -0.37 | 1.61 | 1.41 |
| **Distribution** | | | | |
| BBB permeability (log BB) | -1.58 | -1.71 | 0.446 | -0.08 |
| VDss for humans (log L/kg) | 0.16 | -0.18 | 0.29 | -0.11 |
| CNS permeability (log PS) | -3.32 | -4.72 | -2.38 | -1.70 |
| **Metabolism** | | | | |
| CYP2D6 inhibitor | Inactive | Inactive | Inactive | Inactive |
| CYP2E1 inhibitor | Inactive | Inactive | Inactive | Inactive |
| CYP3A4 inhibitor | Inactive | Inactive | Active | Inactive |
| CYP2C9 inhibitor | Active | Inactive | Inactive | Inactive |
| CYP2C19 inhibitor | Active | Inactive | Inactive | Inactive |
| CYP1A2 inhibitor | Active | Inactive | Inactive | Inactive |
| **Excretion** | | | | |
| Total clearance (log mL/min/kg) | 0.47 | 0.64 | 1.09 | 0.54 |
| Renal OCT2 substrate | No | No | Yes | No |

| | | | | |
|---|---|---|---|---|
| **Toxicity** | | | | |
| Cytotoxicity | Inactive | Inactive | Inactive | Active |
| Mutagenicity | Active | Inactive | Inactive | Inactive |
| Cardiotoxicity | Inactive | Inactive | Inactive | Inactive |
| Hepatoxicity | Inactive | Inactive | Inactive | Inactive |
| hERG inhibitor I | Inactive | Inactive | Inactive | Inactive |
| hERG inhibitor II | Inactive | Active | Inactive | Active |
| LD50 (mol/kg) | 2.84 | 2.92 | 1.65 | 2.34 |

For excretion, the total clearance values were moderate, and petasitolone was identified as a substrate for the renal transporter OCT2. Toxicity assessment indicated that most parameters were inactive in terms of cytotoxicity, except for stigmastane-3,6-dione; mutagenicity, except for quercetin; and cardiotoxicity. All compounds were inactive against hERG I, while some were active against hERG II, namely guaijaverin and stigmastane-3,6-dione, which may raise concerns regarding cardiac safety. The LD50 values indicated moderate toxicity, with guaijaverin showing the highest tolerance at 2.92 mol/kg. Therefore, quercetin, guaijaverin, petasitolone, and stigmastane-3,6-dione have potential for development as therapeutic agents, although further optimization is needed to address potential safety issues.

## Molecular Dynamics Simulation

Molecular dynamics simulations were performed to further validate the stability of the best protein–ligand complexes identified from molecular docking and binding pocket analysis. In this study, only the best ligand from each target protein was selected for molecular dynamics simulation. Stigmastane-3,6-dione was selected for PfDHFR-TS because it showed the strongest binding affinity among all tested compounds, with a docking score of −10.4 kcal/mol, and was able to occupy the active binding pocket of PfDHFR-TS. Meanwhile, quercetin was selected for PfLDH because it showed one of the strongest binding affinities, with a docking score of −8.0 kcal/mol, and properly occupied the catalytic binding pocket of PfLDH. Chloroquine was also included in the molecular dynamics simulation as a positive control to compare the dynamic stability of the selected natural compounds with that of a known antimalarial reference compound. The molecular dynamics simulation of PfDHFR-TS with chloroquine and stigmastane-3,6-dione is presented in **Figure 5**.

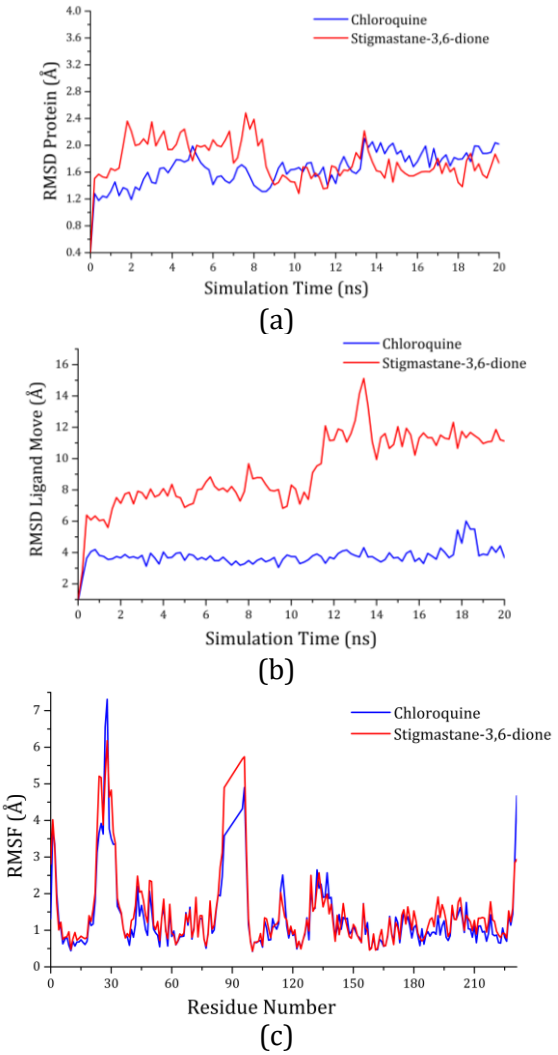


**Figure 5**. Molecular dynamics simulation of PfDHFR-TS with chloroquine and stigmastane-3,6-dione: (a) RMSD Cα, (b) ligand RMSD, and (c) RMSF.

For the PfDHFR-TS complex, RMSD analysis of Cα atoms showed that the chloroquine–PfDHFR-TS complex had RMSD values ranging from approximately 1.17 to 2.10 Å after the initial equilibration phase (see **Figure 5a**). This indicates that the protein backbone remained stable throughout the 20 ns simulation. Similarly, the stigmastane-3,6-dione–PfDHFR-TS complex showed RMSD values ranging from approximately 1.28 to 2.48 Å. Although stigmastane-3,6-dione showed slightly higher fluctuations during the early simulation phase, the RMSD values remained below 3 Å, indicating that the overall protein structure was not significantly destabilized by ligand binding. This suggests that the PfDHFR-TS protein maintained good conformational stability in both the chloroquine and stigmastane-3,6-dione complexes.

However, ligand movement RMSD showed a different trend (see **Figure 5b**). Chloroquine exhibited relatively stable ligand movement, mostly ranging from 3.0 to 4.5 Å, with a maximum value of 6.01 Å. In contrast, stigmastane-3,6-dione showed much higher ligand movement, increasing from approximately 6–9 Å in the early simulation period to a maximum value of 15.11 Å. This high ligand RMSD indicates that stigmastane-3,6-dione experienced substantial positional rearrangement during the simulation. Therefore, although stigmastane-3,6-dione showed the best docking score, its binding pose was less stable under dynamic simulation conditions compared with chloroquine. This finding suggests that the docking result of stigmastane-3,6-dione should be interpreted carefully because its strong binding affinity may not fully represent long-term positional stability in the binding pocket.

Root-mean-square fluctuation (RMSF) analysis of PfDHFR-TS showed that most residues in both complexes had fluctuation values below 2 Å, indicating good structural rigidity of the protein (see **Figure 5c**). Higher fluctuations were observed mainly in flexible loop and terminal regions, particularly around residues 23–32, 84–97, and 230–231. Importantly, key residues involved in ligand interaction, such as Ile14, Cys15, Leu46, Ser111, Val168, and Tyr170, showed relatively low RMSF values. This indicates that the active site region of PfDHFR-TS remained structurally stable during the simulation, even though stigmastane-3,6-dione showed high ligand movement.

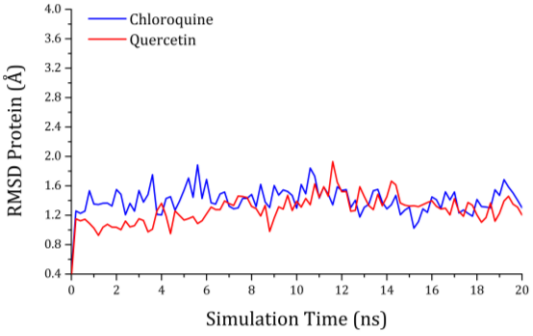


(a)

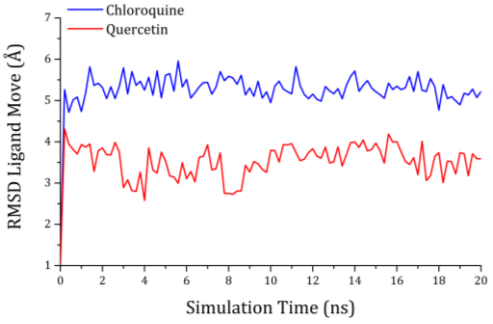


(b)

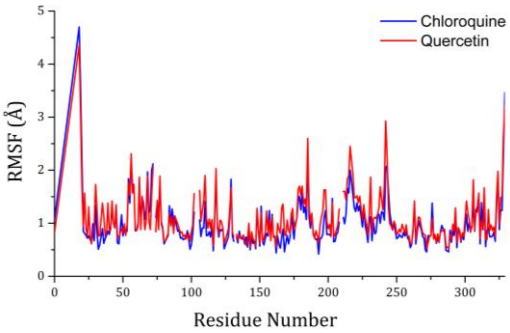


(c)

**Figure 6**. Molecular dynamics simulation of PfLDH with chloroquine and quercetin: (a) RMSD Cα, (b) ligand RMSD, and (c) RMSF.

Furthermore, the molecular dynamics simulation of PfLDH with chloroquine and quercetin is presented in **Figure 6**. For the PfLDH complex, RMSD analysis of Cα atoms demonstrated that both chloroquine and quercetin maintained stable protein conformations during the 20

ns simulation. The chloroquine–PfLDH complex showed RMSD values ranging from approximately 1.02 to 1.88 Å, while the quercetin–PfLDH complex ranged from approximately 0.92 to 1.93 Å after equilibration (see **Figure 6a**). These values remained below 2 Å for most of the simulation period, indicating that both complexes maintained strong protein backbone stability. Compared with the PfDHFR-TS complex, the PfLDH complexes showed lower protein RMSD values, suggesting more stable global conformational behavior.

Ligand movement RMSD analysis further supported the stability of quercetin in the PfLDH binding pocket (see **Figure 6b**). Chloroquine showed ligand RMSD values predominantly around 5.0–5.9 Å, with a maximum value of 5.96 Å. In contrast, quercetin showed lower ligand movement, mostly ranging from 2.7 to 4.1 Å, with a maximum value of 4.31 Å. This indicates that quercetin maintained a more stable position in the PfLDH binding pocket compared with chloroquine. The relatively lower ligand movement of quercetin supports the docking and binding pocket results, in which quercetin was shown to interact with important catalytic residues such as Gly99, Asn140, and Thr139.

RMSF analysis of PfLDH showed that most residues in both the chloroquine and quercetin complexes had fluctuation values below 2 Å, indicating overall residue stability (see **Figure 6c**). Higher fluctuations were mainly found in terminal and flexible loop regions, especially around residues 18–20 and 328–329. In the quercetin complex, several local fluctuations were also observed around residues 185, 216, 242, and 328–329. However, key catalytic residues involved in quercetin binding, such as Gly99, Thr139, Asn140, and Pro250, showed relatively low RMSF values, indicating that the catalytic pocket remained stable during the simulation.

Overall, molecular dynamics simulations demonstrated that both selected natural compounds maintained protein structural stability in their respective target complexes. Stigmastane-3,6-dione was able to maintain the overall stability of PfDHFR-TS, although its high ligand movement suggests lower positional stability within the binding pocket. In contrast, quercetin showed both stable protein RMSD and relatively low ligand movement in the PfLDH complex, indicating better dynamic stability compared with chloroquine. Therefore, quercetin appears to be dynamically more stable as a PfLDH inhibitor candidate, while stigmastane-3,6-dione remains promising for PfDHFR-TS but may require further structural optimization to improve its binding persistence.

## Conclusion

This study evaluated the antimalarial potential of *P. guajava* L. leaf metabolites against two essential *P. falciparum* enzymes, PfDHFR and PfLDH, through an integrated computational workflow consisting of target validation, PASS-based bioactivity prediction, molecular docking, binding pocket validation, molecular dynamics simulation, and ADMET analysis. Preliminary bioactivity prediction indicated that several compounds exhibited relatively low Pa values, suggesting that their antimalarial potential required further structural validation through molecular simulation approaches.

Molecular docking analysis demonstrated that several compounds showed stronger binding affinity than chloroquine (−7.1 kcal/mol), particularly stigmastane-3,6-dione against PfDHFR (−10.4 kcal/mol) and quercetin against PfLDH (−8.0 kcal/mol). However, binding pocket validation revealed that high docking affinity alone was insufficient to determine inhibitory potential. Although hyptatic acid exhibited strong binding energy toward PfLDH, it interacted outside the catalytic pocket, indicating possible false-positive docking behavior and reducing its likelihood as a competitive inhibitor.

Molecular dynamics simulation further confirmed that the quercetin–PfLDH complex exhibited better structural stability and ligand retention compared with

chloroquine, supporting its role as a promising competitive inhibitor. Meanwhile, stigmastane-3,6-dione remained the most favorable PfDHFR candidate due to its strong binding affinity and optimal occupation of the catalytic pocket. ADMET analysis revealed that quercetin, guaijaverin, petasitolone, and stigmastane-3,6-dione possessed promising pharmacokinetic characteristics, although several toxicity-related limitations still require optimization. Overall, quercetin and stigmastane-3,6-dione emerged as the most promising lead compounds for further *in vitro* and *in vivo* antimalarial development.

## Acknowledgement

This work was funded by a Collaborative Grant from the Faculty of Mathematics and Natural Sciences, Universitas Islam Indonesia, under Contract Number 598/Dek-FMIPA/70/MIPA/VIII/2025.

## References

[1] Venkatesan, P. 2025. WHO world malaria report 2024, *Lancet Microbe*. 6. 101073. https://doi.org/10.1016/j.lanmic.2025.101073

[2] World Malaria Report. 2024. *Addressing Inequity in the Global Malaria Response*; World Health Organization: Geneva. Accessed from https://www.who.int/teams/global-malaria-programme/reports/world-malaria-report-2024 at 18-01-2026. There is no corresponding record for this reference.

[3] Fidock, D. A., Rosenthal, P. J. 2021. Artemisinin Resistance in Africa: How Urgent Is the Threat?. *Med, 2* (12), 1287–1288. https://doi.org/10.1016/j.medj.2021.11.005

[4] Noreen, N., Ullah, A., Salman, S. M., Mabkhot, Y., Alsayari, A., Badshah, S. L. 2021. New Insights into the Spread of Resistance to Artemisinin and Its Analogues. *J. Glob Antimicrob Resist*, *27*, 142–149. https://doi.org/10.1016/j.jgar.2021.09.001

[5] Balikagala, B., Fukuda, N., Ikeda, M., Katuro, O.T., Tachibana, S.L., Yamauchi, M., Opio, W., Emoto, S., Anywar, D.A., Kimura, E., Palacpac, N.M.Q., Odongo-Aginya, E.I., Ogwang, M., Horii, T., Mita. T. 2021. Evidence of Artemisinin-Resistant Malaria in Africa. *N Engl J. Med. 385* (13), 1163–1171. https://doi.org/10.1056/NEJMoa2101746

[6] Dhorda, M., Kaneko, A., Komatsu, R., Mshamu, A. Kc. S., Gesase, S., Kapologwe, N., Assefa, A., Opigo, J., Adoke, Y., Ebong, C. 2024. Artemisinin-resistant malaria in Africa demands urgent action. *Science*, 385, 252–254. https://doi.org/10.1126/science.adp5137

[7] Kamya, M.R., Nankabirwa, J.I., Ebong, C., Asua, V., Kiggundu, M., Orena, S., Okitwi, M., Tukwasibwe, S., Agaba, B., Kyabayinze, D., Opigo, J. 2025. Efficacies of artemether– lumefantrine, artesunate–amodiaquine, dihydroartemisinin–piperaquine, and artesunate–pyronaridine for the treatment of uncomplicated Plasmodium falciparum malaria in children aged 6 months to 10 years in Uganda: a randomised, open-label, phase 4 clinical trial. *Lancet. Infect. Dis*., 26(1), 67-78. https://doi.org/10.1016/S1473-3099(25)00407

[8] Dondorp, A.M. 2026. Diversifying antimalarial treatment for uncomplicated Plasmodium falciparum malaria in Uganda. *Lancet. Infect. Dis.*, *26*(1), 6-8. https://doi.org/10.1016/S1473-3099(25)00416-5

[9] Minwuyelet, A., Yewhalaw, D., Petronio Petronio, G., Di Marco, R., Atenafu, G. 2026. The Effect of Artemether–Lumefantrine Combined with a Single Dose of Primaquine on Plasmodium falciparum Gametocyte Clearance and

Post-Treatment Infectivity to Anopheles arabiensis. *Trop. Med. Infect. Dis.,* *11*(1),19. https://doi.org/10.3390/tropicalmed11010019

[10] Takyi, A., Soma, A., Przybylska, M., Harriss, E., Barnes, K. I., Dahal, P., Guérin, P.J., Stepniewska, K., Carrara, V.I. 2025. Efficacy of artemisinin-based combination therapy (ACT) in people living with HIV (PLHIV) diagnosed with uncomplicated Plasmodium falciparum malaria in Africa. *Malar. J.,* 11 (1), *24*, 153. https://doi.org/10.1186/s12936-025-05393-8

[11] Hariyanti, H., Mauludin, R., Sumirtapura, Y.C., Kurniati, N.F. 2022. A review: Pharmacological activities of quinoline alkaloid of Cinchona sp. *Biointerface Research in Applied Chemistry*, *13*(4), 1-13. https://doi.org/10.33263/BRIAC134.319

[12] Tafur, E. Cuchca, S., García, L., Rojas-Briceño, N.B., Veneros, J. 2025. Generalized Linear Models to Estimate the Probability of Occurrence of Cinchona officinalis L., Cinchona pubescens Vahl, and Cinchona calisaya Wedd in Peru. *J. Sustain. For.*, *44*(1–5), 103-125. https://doi.org/10.1080/10549811.2025.2513230

[13] Yin, Q., Xiang, L., Han, X., Zhang, Y., Lyu, R., Yuan, L., Chen, S. 2025. The evolutionary advantage of artemisinin production by Artemisia annua. *Trends Plant Sci.*, *30*(2), 213-226. https://doi.org/10.1016/j.tplants.2024.09.006

[14] Roesch, C., Ashraf, K., Vantaux, A., Marin, A.A., Maher, S.P., Franetich, J.F., Kloeung, N., Ke, S., Vo, H.T.M., Barale, J.C., Mazier, D. 2025. Assessment of the in vitro activity and selectivity of Artemisia afra and Artemisia annua aqueous extracts against artemisinin-resistant Plasmodium falciparum. *Malar. J.*, *24*(1),150. https://doi.org/10.1186/s12936-025-05375-w

[15] Belyagoubi-Benhammou, N., Zitouni-Nourine, S.H., Belyagoubi, L., Hedeili, N., Di Marco, G., D'Agostino, A., Gismondi, A., Canini, A. 2025. Exploring isolation protocols for artemisinin and other bioactive compounds from the algerian Artemisia campestris. *Pl. Biosystems, 159*(5), 1114-1128. https://doi.org/10.1080/11263504.2025.2525875

[16] Morua, E., Cuyas,L., Matías-Hernández, L. 2025. The Beneficial Use of Artemisia annua, Artemisinin, and Other Compounds in Animal Health. *Animals*, *15*(10), p.1359. https://doi.org/10.3390/ani15101359

[17] Mukusheva, G.K., Toigambekova, N.N., Seidakhmetova, R.B., Jalmakhanbetova, R.I., Babakhanova, M.N., Nurkenov, O.A., Akishina, E.A., Dikusar, E.A., Kolesnik, I.A., Zhou, H., Potkin, H.V.I. 2025. Synthesis and Biological Activity of Novel Polyazaheterocyclic Derivatives of Quinine. *Molecules*, *30*(15), 3301. https://doi.org/10.3390/molecules30153301

[18] Basrani, S., Patil, S., Chougule, S., Kotalagi, T., Yankanchi, S., Karuppayil, S.M., Jadhav, A.K. 2025. Repurposing of quinine as an antifungal antibiotic: Identification of molecular targets in Candida albicans. *Folia Microbiol.*,1-11. https://doi.org/10.1007/s12223-025-01281-5

[19] Prakoso, N.I., Zakiyah, Z.N., Liyanita, A., Rubiyanto, D., Fitriastuti, D., Ramadani, A.P., Kamari, A., Mow, S.K. 2019. Antimalarial Activity of Andrographis Paniculata Ness's N-hexane Extract and Its Major Compounds. *Open Chemistry*, *17*(1), 788-797. https://doi.org/10.1515/chem-2019-0086

[20] Usman, U., Masruhim, M.A., Rahmadani, A., Erwin, E. 2025. Phytochemistry, Toxicity, and Antimalaria Activity of Mangrove Plant from Muara Badak Beach, East Kalimantan, Indonesia. *Biol. Med. Natural Prod. Chem.*, *14*(1),567-573.

https://doi.org/10.14421/biomedich.2025.141.567-573

[21] Corry, M.N., Ilmi, H., Tumewu, L., Nisa, H.K., Wicaksana, F., Pamungkas, I.R., Salam, S., Kuncoro, H. Suciati, S., Osman, C.P., Hafid, A.F. 2025. Antimalarial and Cytotoxic Activities of Cratoxylum sumatranum (Jack) Bl. Twigs Dichloromethane Extract and Its Phytochemical Profiling by LC-MS/MS. *Trends Sci.*, *22*(10),10576-10576. https://doi.org/10.48048/tis.2025.10576

[22] Tumewu, L. Ilmi, H., Kartika Sari, D., Permanasari, A.A., Khairun Nisa, H., Saputri, R.D., Tjahjandarie, T.S., Tanjung, M., Osman, C.P., Ismail, N.H., Suciati. 2025. Three new dihydrochalcones from the leaves of Artocarpus sericicarpus Jarrett and their activity against Plasmodium falciparum. *Nat. Prod. Res.*, 39(13), 3721-3729. https://doi.org/10.1080/14786419.2024.2308726

[23] Sari, R.K., Syafii, W., Prayogo, Y.H., Carolina, A., Familasari, S., Cahyaningsih, U., Sa'diah, S., Wahyudi, S.T., Lubis, M.A.R., 2025. In Vitro and Molecular Docking Studies of the Antimalarial Activities of Strychnos ligustrina Extracts from Different Parts of the Woody Stem. *J. Korean Wood Sci. Techno*., *53*(1), 89-104. https://doi.org/10.5658/WOOD.2025.53.1.89

[24] Umezawa, T., Prakoso, N.I., Kannaka, M., Nogata, Y., Yoshimura, E., Okino, T., Matsuda, F. 2019. Synthesis and Structure− Activity Relationship of Omaezallene Derivatives, *Chem. Biodivers.*, 16(1), 1-13. https://doi.org/10.1002/cbdv.201800451

[25] Umezawa, T., Prakoso, N.I., Tsuji, K., Ogura, Y., Sato, T., Matsuda, F. 2022. Model Study toward Total Synthesis of Mytilipin C, *Bulletin of the Chemical Society of Japan,* 95(10),1491-1500. https://doi.org/10.1246/bcsj.20220196

[26] Phan, C.S., Ling, Z., Mehjabin, J.J., Matsuda, K., Prakoso, N.I., Umezawa, T., Wakimoto, T., Okino, T. 2024. Doubly Homologated Tyrosine-Containing Peptides from the Cyanobacterium Microcystis aeruginosa NIES-4285 and Their Biosynthesis. *J. Nat. Prod*. 87(11), 2629–2639. https://doi.org/10.1021/acs.jnatprod.4c00972

[27] Prakoso, N.I., Nita, M.T. 2023. Exploring anticancer activity of the Indonesian guava leaf (Psidium guajava L.) fraction on various human cancer cell lines in an in vitro cell-based approach. *Open Chemistry*, 21(1), p.20230101. https://doi.org/10.1515/chem-2023-0101

[28] Umezawa, T., Maeda, T., Akiyama, T., Prakoso, N.I., Mehjabin, J.J., Okino, T., Matsuda, F. 2023. Syntheses and Biological Activities of Danicalipin A Derivatives. *Chem. Biodivers*, 20(6),p.e202300400. **https://doi.org/10.1002/cbdv.202300400**

[29] Prakoso, N.I., Umezawa, T., Rubiyanto, D., Kusumo, A.Z., Septianingtyas, F., Nurochman, M.I., Kristianti, L. Salmahaminati, Jumaryatno, P., Abe, M. 2026. Unveiling the Anticancer Properties of New Synthesized Alkoxy-and Methyl Thio-Chalcone Derivatives. Natural Sciences, 6 (2), e70059. **https://doi.org/10.1002/ntls.70059**

[30] Prakoso, N. I., Matsuda, F., Umezawa, T., 2021. Efficient Synthesis of α,β-Dichlorinated Ketones from α,β-Dichlorinated Weinreb Amides through a Simple Work-up Procedure. *Organic & Biomolecular Chemistry*, 19, 36, 7822-7826. https://doi.org/10.1039/D1OB01379C

[31] Kobayashi, S., Prakoso, N. I., Zheng, X., Noro, S. I., Hashimoto, M., Morozumi, T., Umezawa, T., 2024. Synthesis and Conformational Analysis of α, β-Dichlorocarbonyl Compounds. *European Journal of Organic Chemistry,* 27, 33, p.e202400489 1-7.

https://doi.org/10.1002/ejoc.202400489

[32] Yuan, J., Prakoso, N. I., Morozumi, T., Umezawa, T., 2024. Mild Metal-Free 1, 2-Dichlorination of Alkynes by NCS-$PPh_3$-$H_2O$ System. *Synthesis*, 56, 5, 771-776. https://doi.org/10.1055/a-2218-7443.

[33] Okumura, H., Prakoso, N. I., Morozumi, T., Umezawa, T. 2024. Chemoselective Preparation of Alkynes from Vicinal and Geminal Dibromoalkenes. *Organic letters*, *26*(46), 9817-9821. https://doi.org/10.1021/acs.orglett.4c03483

[34] Prakoso, N. I., Nugroho, N. V., Rubiyanto, D., 2020. Comparative study of the effectiveness of $Na_2CO_3$ and $K_2CO_3$ as base in methylation reaction on eugenol using dimethylcarbonate. *AIP Conference Proceedings*, 2229, 1, 030001. https://doi.org/10.1063/5.0002543

[35] Prakoso, N. I., Pangestu, P. H., Wahyuningsih, T. D., 2016. O-methylation of natural phenolic compounds based on green chemistry using dimethyl carbonate. *IOP Conference Series: Materials Science and Engineering,* 107, 012065. https://doi.org/10.1088/1757-899X/107/1/012065

[36] Cavasotto, C.N., Di Filippo, J.I. 2021. In silico drug repurposing for COVID-19: Targeting SARS-CoV-2 proteins through docking and consensus ranking. *Mol. Inform*. 40(1), 2000115. https://doi.org/10.1002/minf.202000115

[37] Purwiandono, G., Nabila, N., Busro, M., Salmahaminati, S., Wicaksono, W. P., Prakoso, N. I., Utami, M. 2026). Examining active compounds in ginger as a potential treatment for respiratory syndrome: A molecular docking and dynamics study. In *BIO Web of Conferences* (Vol. 226, p. 03004). EDP Sciences. https://doi.org/10.1051/bioconf/202622603004

[38] Heikal, M.F., Putra, W.E., Sustiprijatno, Rifa'I, M., Hidayatullah, A., Ningsih, F.N., Widiastuti, D., Shuib, A.S., Zulfiani, B.F., Hanasepti, A.F. 2023. In Silico Screening and Molecular Dynamics Simulation of Potential Anti-Malarial Agents from *Zingiberaceae* as Potential *Plasmodium falciparum* Lactate Dehydrogenase (PfLDH) Enzyme Inhibitors. Trop. Life Sci. Res., 34(2), (2023), 1-20. https://doi.org/10.21315/tlsr2023.34.2.1.

[39] Suresh, P.S., Kesarwani, V., Kumari, S., Shankar, R., Sharma, U. 2023. Flavonoids from aerial parts of Cissampelos pareira L. as antimalarial agents: Computational validation of ethnopharmacological relevance. *S. Afr. J. Bot.* 163, 10-19. https://doi.org/10.1016/j.sajb.2023.10.017

[40] Bibi, A., Maryem, A., Mushtaq, S.M., Iqbal, A., Shaheen, L., Hani, U., Hameed, A., Fatima, M., Rasool, M., Muqaddas, H. 2025. Medicinal Plants against Malaria and Dengue: In-Silico Computational Drug Discovery Framework for Identifying Therapeutic Leads. *MAP.*, 25(22), 142-150. https://doi.org/10.47278/book.HH/2025.453

[41] Volkamer, A., Griewel, A., Grombacher, T., Rarey, M. 2010. Analyzing the Topology of Active Sites: On the Prediction of Pockets and Subpockets, *J. Chem. Inf. Model*, 50 (11), 2041-2052. https://doi.org/10.1021/ci100241y

[42] Volkamer, A., Kuhn, D., Grombacher, T., Rippmann, F., Rarey, M. 2012. Combining Global and Local Measures for Structure-Based Druggability Predictions, *J. Chem. Inf. Model*, 52 (2), 360-372. https://doi.org/10.1021/ci200454v

[43] Oktriawan, T., Aulia, B.A., Setyawan, T., Raharjo, T.J., Haryadi, W., Commeiras, L., Mardjan, M.I.D. 2025. Quinazolinone Derivatives as Targeting pfDHFR and pfDHODH Inhibitor: In Silico Studies Using Molecular Docking, Molecular

Dynamics Simulations, MM-PBSA, and ADMET Analysis, *Trends Sci.*, 23 (1), 11331. https://doi.org/10.48048/tis.2026.11331

[44] Thomas, T.V., Thakur, A., Kumar, S.A., Krishnan, A. 2025. Inhibition Mechanism and Target Reassessment of Potent Piperaquine Analogs: Evidence for PfLDH over PfDHODH, *ACS Omega*, 10 (49), 60435-60449. https://doi.org/10.1021/acsomega.5c07677